Journal of Applied Electrochemistry **32**: 653–660, 2002.

Influence of power ultrasound on the corrosion of aluminium and high speed steel

N.L.P.A. DE MORAIS and C.M.A. BRETT*
Departamento de Química, Universidade de Coimbra, 3004-535 Coimbra, Portugal
*(*author for correspondence, fax: +351 239 835295, e-mail: brett@ci.uc.pt)*

Received 13 February 2002; accepted in revised form 1 May 2002

Key words: aluminium, corrosion, high speed steel, ultrasound

Abstract

The influence of power ultrasound on the corrosion of aluminium and high speed steel in chloride medium has been investigated. Open circuit potential, polarization curves and electrochemical impedance spectroscopy were employed to study the corrosion process before, during and after ultrasonic irradiation as well as scanning electron microscopy of the corroded surfaces. Cavitation led to formation of pits, erosion and increased mass transport. The effect of ultrasound power, chloride concentration, horn tip–metal distance and of tip diameter were assessed. The principal effect of ultrasound on aluminium is destruction of the oxide film and on high speed steel removal of corrosion products and increased solution mass transport; the influence of ultrasound is greatest at low chloride concentrations. For both metals it was shown that for chloride ion concentrations up to 0.1 M the influence of ultrasound power is most evident, followed by the distance between probe tip and metal, then [Cl^-] and lastly the size of the probe tip. The potentialities of using ultrasound as a rapid diagnostic test of corrosion resistance are indicated.

1. Introduction

As early as the 1930s, the depolarizing effect of ultrasound was recognized [1, 2]. Sonication has been used to increase the electroanalytical current [3], to improve quality in electroplating [4, 5] and for electrode pretreatment [6]. More recently, there has been much attention paid to the fundamental understanding of sonoelectrochemical processes and to new, diverse applications, for example in synthesis and analysis [7, 8].

In chemistry, ultrasound is known for its capacity to promote heterogeneous reactions [9] mainly through mass transport enhancement, surface cleaning and thermal effects. Corrosion as an interfacial process, depends very much on all three of these parameters.

A number of recent studies have been undertaken concerning the influence of ultrasound on the erosion and corrosion of different metal surfaces. The electrochemical behaviour of zinc in aqueous sodium hydroxide solution under the application of 20 kHz power ultrasound was investigated, leading to the conclusion that there is a synergistic effect between the ultrasound and corrosion [10]. The cavitation–erosion resistance of a variety of metals has been assessed through the application of bursts of 20 kHz ultrasound every 30 min over a 4 h period in 3.5% NaCl by Man et al. [11]. The corrosion resistance, from polarization curves, and pure mechanical erosion were both measured separately and compared with cavitation-induced erosion and corrosion occurring together. It was shown that there can be a significant synergistic effect, of the metals studied particularly grey cast iron and 1050 mild steel. The synergistic effect for erosion- and cavitation–corrosion of titanium and its alloys was also demonstrated [12].

Man et al. also investigated laser-alloyed coatings of about 0.15 mm thickness on a number of different metallic substrates using once again a 20 kHz ultrasonic probe in 3.5% NaCl solution. These included mild steel [13–15], stainless steel [13, 14, 16, 17], aluminium alloy [18, 19] and brass [20]. The open circuit potential was monitored throughout the process and showed abrupt changes on switching on and off the ultrasound source.

Soyama and Asahara [21] found that the corrosion resistance of a carbon steel surface was improved and reached a stable value of open circuit potential faster following impingement of a cavitating jet in water, which had caused erosion of the steel and had cleaned the steel surface. When the metal itself was made to oscillate (being an aluminium plate in [22]) — it was seen that the erosion is uniform at short times, becoming nonuniform and worse at the centre of the plate at long times.

The objective of this work was to study the effect of 20 kHz power ultrasound on the electrochemical behaviour and corrosion of aluminium and of high speed steel in chloride solution. The reason for the choice of these two metals was that they show different characteristics with regard to oxide film formation, as shown in

previous studies [23, 24]. Important aspects investigated concerned the influence of ultrasound on the corrosion mechanism, particularly of mass transport, the surface cleaning effect, enhancement of corrosion through cavitation and the ease of re-formation of any protective oxide layer.

2. Experimental details

The metals employed were 99.99% pure aluminium and annealed AISI M2 high speed steel (composition W 6.4, Mo 5.0, Cr 4.2, V 1.9, C 0.9 percentage by weight). These were in the form of discs, circular surface area 0.28 cm^2 and 0.95 cm^2, respectively, and were made into electrodes by attaching a copper wire to one face with silver conducting epoxy and, when dry, covering this and the rest of the metal except for one face with ordinary epoxy resin. Electrodes were carefully polished, before each experiment, using silicon carbide abrasive paper, down to 1200 grade. A platinum spiral served as counter electrode and a saturated calomel electrode (SCE) was used as reference. A thermostatted cell with 150 cm^3 solution was employed in all experiments. The electrolyte used was KCl (Merck *pro analysi*) in three different concentrations: 0.01, 0.1 and 1 M, made with Milli-Q ultrapure water (resistivity >18 MΩ cm).

Electrochemical experiments were conducted with a PAR 273A potentiostat running M352 corrosion analysis software for open circuit potential (OCP) and polarization curves. The scan rate used was 5 mV s^{-1} and the potential limits were ± 0.200 V vs OCP. The polarization curves were analysed with ParCalc in the M352 software.

Electrochemical impedance experiments were carried out using a Solartron 1250 frequency response analyser coupled to a Solartron 1286 electrochemical interface, controlled by ZPlot software (Scribner Associates). An r.m.s. sinusoidal potential perturbation of 10 mV was applied and frequencies were scanned from 65 KHz to 0.1 Hz. Spectra were fitted to equivalent circuits with ZSim software (Scribner Associates).

Ultrasound was applied using a Vibra cell 501 model sonic horn (Sonics & Materials) working at 20 kHz with a titanium-tipped probe. Two different kind of tips were used, one with 3 mm diameter (microtip) and the other with 10 mm diameter. Power levels of 22, 30 and 44 W cm^{-2} were used, as calibrated by the calorimetric method described in [23]. A thermostat (Haake D3) was used to keep the electrochemical cell at 25 °C. To keep the temperature as constant as possible, sonication was normally applied for only five minutes and pulses of two seconds were used (2 s on, 1 s off).

In experiments involving measurement of open circuit potential, ultrasound was applied between 15 and 20 min following immersion. For the registering of polarization curves and impedance spectra, ultrasound was applied for a 5 min period beginning one minute after registering the curve or spectrum after 10 min immersion. Polarization curves and spectra were recorded 10, 25 and 60 min after the initial immersion when a sufficiently good steady state had been reached such that the corrosion potential was almost invariant over the timescale of the experiment.

3. Results and discussion

3.1. *Method of application of ultrasound pulses*

A preliminary study of the best way to apply ultrasound was carried out, in order to compromise between a significant effect on the corrosion process and minimization of the heating effect of ultrasound on prolonged application. Pulses were applied for different time periods from 2 to 60 s over a 5 min period, with a one second interval between pulses. The open circuit potential was monitored continuously before and after ultrasound irradiation up to a total of 1 h immersion.

Typical results for high speed steel are shown in Figure 1. As can be seen, and as was also found for aluminium, the most significant change, and with the least heating effect, was with 2 s pulses. These conditions, cycles of 2 s on and 1 s off, were used in all the experiments described below.

3.2. *Open circuit potential*

Open circuit potentials were measured under a variety of conditions over a period of 1 h, applying ultrasound (2 s on, 1 s off) during 5 min from 15 to 20 min after initial immersion. All possible parameters were varied, which included ultrasound power, probe size, distance between probe and metal surface and chloride concentration. The type of response for aluminium is shown in Figure 2 as a function of probe diameter and chloride concentration and the same is shown for high speed steel in Figure 3.

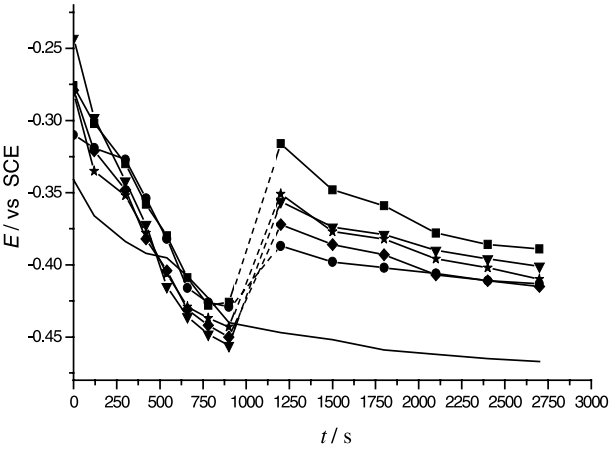

Fig. 1. Effect of ultrasound on the open circuit potential of high speed steel, applied between 900 and 1200 s after immersion, for different pulse lengths and one second rest period between pulses: 3 mm probe at 1.0 cm from steel surface, power 44 W cm^{-2}, $[Cl^-] = 0.01$ M. Key: (—) no ultrasound; pulse: (■) 2, (●) 5, (▼) 10, (♦) 30 and (★) 60 s.

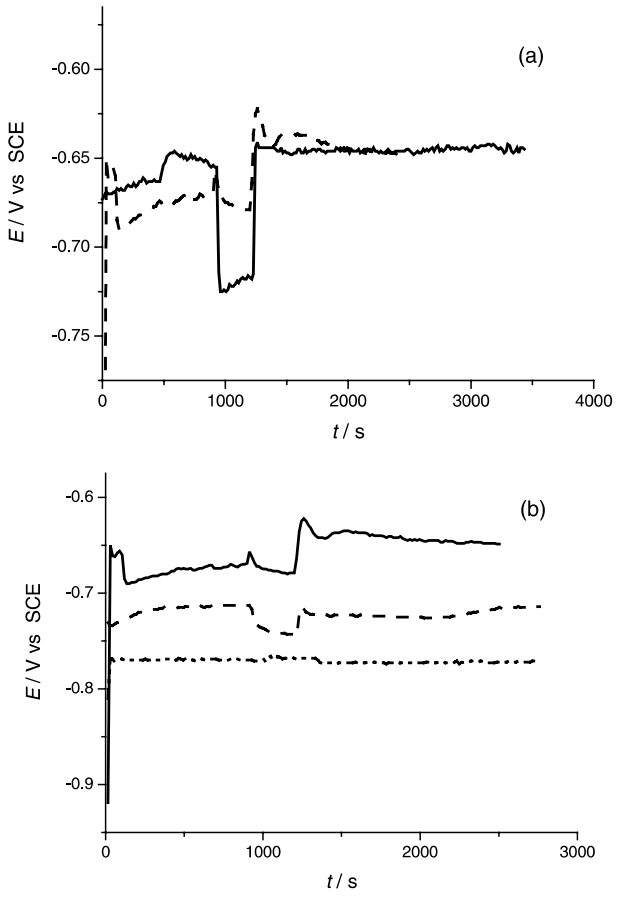

Fig. 2. Variation of open circuit potential of aluminium with time; ultrasound applied between 900 and 1200 s (2 s on + 1 s off); ultrasound power 22 W cm^{-2}, tip–electrode distance 1.0 cm. (a) Influence of tip diameter: (—) 3 mm and (– – –) 10 mm; $[Cl^-] = 0.1$ M. (b) Influence of chloride concentration: (—) 0.01 M, (– – –) 0.1 M and (–··–) 1.0 M. 3 mm diameter tip.

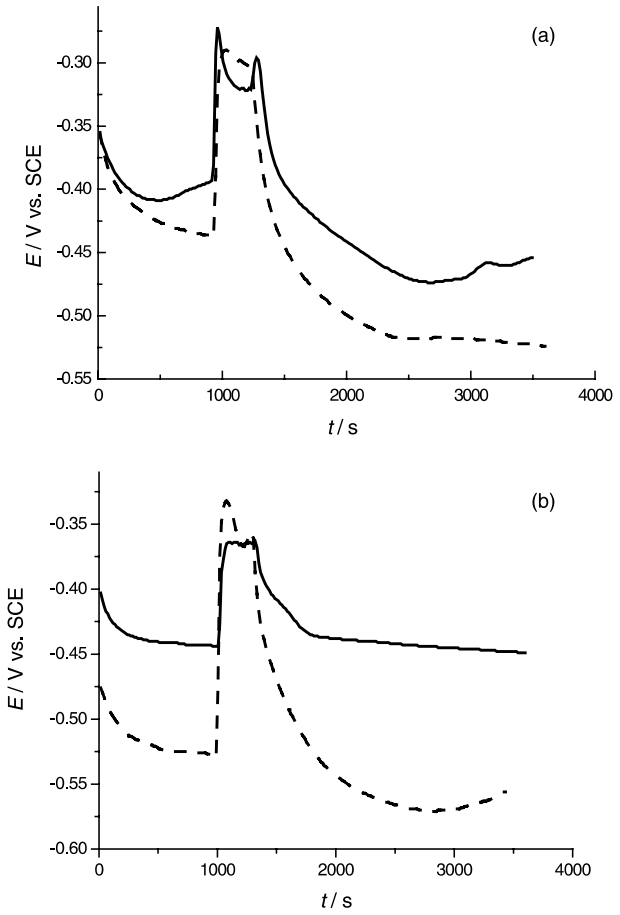

Fig. 3. Variation of open circuit potential of high speed steel with time; ultrasound applied between 900 and 1200 s (2 s on + 1 s off); ultrasound power 22 W cm^{-2}, tip–electrode distance 1.0 cm. (a) Influence of tip diameter: (—) 3 mm and (– – –) 10 mm; $[Cl^-] = 0.1$ M. (b) Influence of chloride concentration: (—) 0.01 M and (– – –) 0.1 M. 3 mm diameter tip.

Figures 2 and 3 show that the initial values of potential before application of ultrasound are not the same; this is common in measurements of open circuit potential and reflects different states of the surface and differences in sample morphology at the submicroscopic level. However, for identical repeat experiments the difference in the potential, ΔE, on commencing irradiation and just before never varied by more than 9 mV, suggesting that the influence of ultrasound is the same.

The open circuit potential for aluminium tends to become more positive after immersion, following initial sharp changes, which can be ascribed to the formation of an oxide film. A fairly constant value was achieved after 10 min immersion. Application of ultrasound to aluminium causes the potential to change abruptly to a more negative value, which can be attributed to destruction of the oxide layer. Figure 2(a) demonstrates that the smaller tipped probe has more influence than the larger-tipped probe. It can be seen in Figure 2(b) that at a concentration of 1.0 M chloride ion ultrasound has no effect on the OCP, which shows that the chloride ion is much more effective in destroying (or preventing formation of) the oxide layer than ultrasound.

In the case of HSS, for which the potential tends to move in the negative direction in the absence of ultrasound, on sonication the variation is to more positive potentials. Here it is well known that oxide is not easily formed. Large potential spikes appear which are probably due to the mass transport effect removing any loosely-bound oxide from the surface. After ceasing to apply ultrasound the open circuit potentials move towards the values before irradiation and appear to continue the previous tendencies. For high speed steel, there is no marked difference between the 3 mm and 10 mm diameter tips, Figure 3(a), which suggests that the erosion of the surface occurrs by a different mechanism from aluminium. These differences between different metals according to their oxide-forming ability have been noted in the studies by Man et al. [11], although their experimental conditions were much more aggressive. The aggressive effect of chloride ion is much more pronounced than with aluminium so that it was not possible to carry out any experiments with 1.0 M chloride without complete surface destruction.

The effect of ultrasound power and probe tip to metal distance are summarized in Table 1. It can be clearly

Table 1. Difference in OCP, ΔE/V, of aluminium and high speed steel just after and before commencing application of ultrasound
Tip diameter 3 mm; [Cl^-] = 0.1 M. Ultrasound applied between 900 and 1200 s (2 s on + 1 s off)

Metallic substrate	Ultrasound power/W cm^{-2} *			Probe-electrode distance/cm†		
	22	30	44	0.5	1.0	1.5
Aluminium	−0.029	−0.045	−0.053	−0.095	−0.037	−0.028
High speed steel	0.113	0.142	0.145	0.184	0.108	0.075

* Tip-electrode distance 1 cm.
† Ultrasound power 22 W cm^{-2}.

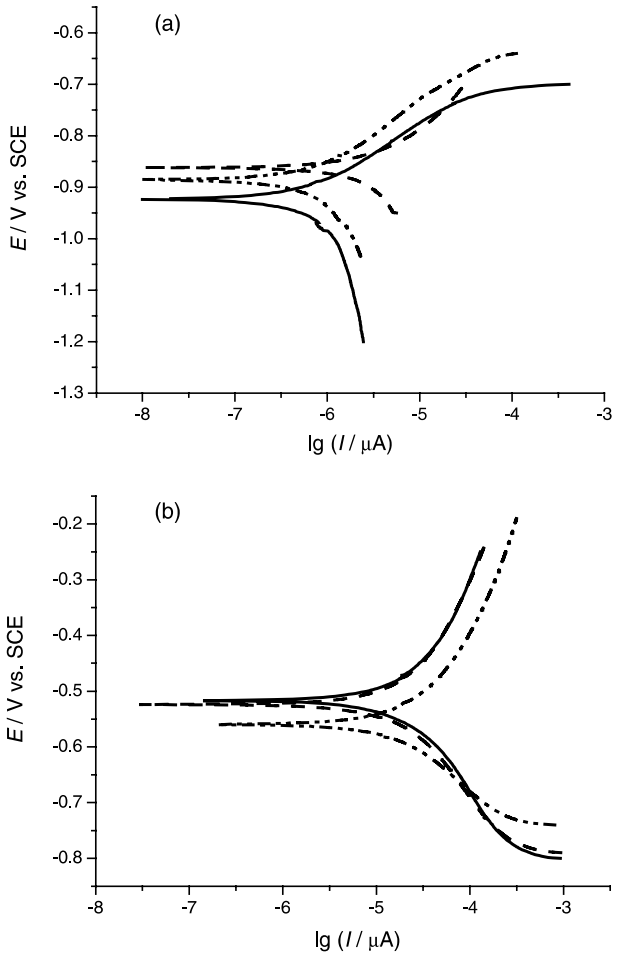

Fig. 4. Polarization curves for (a) aluminium and (b) high speed steel. Immersion times: (—) 10 min, (– – –) 25 min and (–·–) 60 min. Ultrasound applied between 12 and 17 min after immersion (2 s on + 1 s off). Ultrasound power 44 W cm^{-2}, tip–electrode distance 1.0 cm, [Cl^-] = 0.1 M, 3 mm diameter tip.

seen that ultrasound power affects aluminium much less than high speed steel and the distance dependence is also less. It is also reflected in the influence of chloride concentration, which is less for aluminium than for high speed steel and can be traced to a lower corrosion rate. This will be discussed further below.

3.3. *Polarization curves*

Typical polarization curves in the region of the corrosion potential are shown in Figure 4 for aluminium and high speed steel. These were recorded at three different times during the experiment. The first was recorded after 10 min immersion. Immediately following this, ultrasound was applied for 5 min (pulses of 2 s with 1 s interval). The next polarization curve was registered after 25 min when an almost steady-state value of the corrosion potential had once again been reached and finally after 1 h immersion. Of particular interest were comparisons between 10 and 25 min immersion and between 25 and 60 min immersion. Tafel analysis of the curves was carried out and the results are shown in Tables 2 and 3.

Regarding aluminium, the tendency for the currents to reach limiting values at applied potentials negative of the corrosion potential is seen in Figure 4(a) and is in agreement with its oxide-forming ability limited by the cathodic reaction. Increases in current associated with pitting are also evident at about 0.17 V positive of the corrosion potential, as expected. Figure 6(b) shows that for high speed steel the currents are large than for aluminium but there is no specific potential that can be associated with the commencement of pitting.

Tables 2 and 3 show that, in general terms, the corrosion currents parallel the values of corrosion potential. It can also be seen that the initial variation between the different values of corrosion potential before ultrasound is less after its application, suggesting that there has been some rearrangement of the surface structure and morphology. This is what was found in [21] with respect to carbon steel.

The values of the corrosion currents tend to increase after application of ultrasound. After 1 h immersion the values are lower than after 10 min immersion which suggests that the film is thicker or less porous than that formed initially.

3.4. *Electrochemical impedance*

Electrochemical impedance spectra were recorded for aluminium and high speed steel at the corrosion potential after the same immersion times as for the recording of polarization curves. Typical results are shown in complex plane and Bode format in Figures 5 and 6. For the various immersion times, the former brings out differences at low frequencies and the latter enables changes in the high frequency range to be more easily assessed. Inspection shows that differences

Table 2. Values of E_{cor} and I_{cor} for aluminium as a function of the different ultrasound parameters studied

		E_{cor}/V vs SCE			I_{cor}/μA cm^{-2}		
		10 min	25 min	60 min	10 min	25 min	60 min
Tip diameter/mm*	3	−0.921	−0.862	−0.885	1.2	4.9	0.7
	10	−0.843	−0.729	−0.724	4.0	5.1	5.5
Power/W cm^{-2}†	22	−1.016	−0.902	−0.882	1.5	7.3	1.7
	30	−1.025	−0.907	−0.838	2.9	10.5	1.1
	44	−1.052	−1.013	−0.985	3.1	15.8	2.0
Tip–electrode distance/cm‡	1.0	−0.921	−0.862	−0.885	1.2	4.9	0.7
	1.5	−0.940	−0.880	−0.908	0.5	1.6	0.3
[Cl$^-$] / mol dm^{-3}§	0.01	−0.921	−0.862	−0.885	1.2	4.9	0.7
	0.1	−0.915	−0.902	−0.877	3.0	4.9	4.3
	1.0	−1.012	−1.057	−1.070	0.2	8.7	5.3

*[Cl$^-$] = 0.01 M; distance 1.0 cm; power 44 W cm^{-2}.
†[Cl$^-$] = 0.01 M; 3 mm diameter tip; distance 1.0 cm.
‡[Cl$^-$] = 0.01 M; 3 mm diameter tip; power 44 W cm^{-2}.
§3 mm diameter tip; distance 1.0 cm, power 44 W cm^{-2}.

Table 3. Values of E_{cor} and I_{cor} for high speed steel as a function of the different ultrasound parameters studied

		E_{cor}/V vs SCE			I_{cor}/μA cm^{-2}		
		10 min	25 min	60 min	10 min	25 min	60 min
Tip diameter/mm*	3	−0.508	−0.510	−0.558	24.7	27.6	28.7
	10	−0.502	−0.526	−0.520	23.2	24.5	26.0
Power/W cm^{-2}†	22	−0.472	−0.464	−0.554	27.8	31.8	28.5
	30	−0.503	−0.484	−0.567	27.6	35.3	26.8
	44	−0.531	−0.515	−0.573	28.2	41.5	26.6
Tip–electrode distance/cm‡	1.0	−0.529	−0.530	−0.555	27.5	48.5	35.7
	1.5	−0.514	−0.880	−0.557	25.2	35.7	25.6
[Cl$^-$] / mol dm^{-3}§	0.01	−0.529	−0.530	−0.555	27.5	48.5	35.7
	0.1	−0.641	−0.658	−0.695	32.5	58.6	60.5

*[Cl$^-$] = 0.01 M; distance 1.0 cm; power 44 W cm^{-2}.
†[Cl$^-$] = 0.01 M; 3 mm diameter tip; distance 1.0 cm.
‡[Cl$^-$] = 0.01 M; 3 mm diameter tip; power 44 W cm^{-2}.
§3 mm diameter tip; distance 1.0 cm, power 44 W cm^{-2}.

between the three immersion times are greatest at lower frequencies. In the range of frequencies studied, aluminium shows processes with two time constants and high speed steel with only one time constant.

In the case of aluminium, it can be seen that the spectra are similar after 10 and 60 min immersion, but the impedance values are smaller after 25 min, when the system is recovering from the irradiation by ultrasound. On the other hand, with HSS, the spectra show an irreversible change after application of ultrasound suggesting that irreversible changes have taken place on the metal surface.

The spectra were fitted with the circuit shown in Figure 7 for aluminium; for high speed steel, which has only one time constant, the element *DE2* was omitted. The distributed elements were modelled as

$$Z = C^{-1}(i\omega)^{-\alpha}$$

where C is the capacitance, ω the frequency in rad s^{-1} and α the constant phase angle exponent. The physical meaning of this circuit is that for aluminium there are two different types of surface sites which can be attributed to those with a surface oxide layer not undergoing corrosion and those sufficiently attacked by chloride ion that there is pitting associated with some charge separation (see SEM below). For HSS there is no charge separation associated with the pitted areas since there is no tendency for oxide formation at these points. This is in agreement with previous results for HSS. The values of the different fitted parameters are given in Table 4, and there is good agreement over the whole frequency range.

The deductions made in previous Sections regarding reversible and irreversible changes to the interfacial region are here clearer. There is some recovery of the R_{ct} values after 60 min immersion compared with 25 min, following the decrease on comparing 25 min to 10 min immersion (after and before irradiation), suggesting the formation of a film on the surface after application of ultrasound which impedes electron transfer.

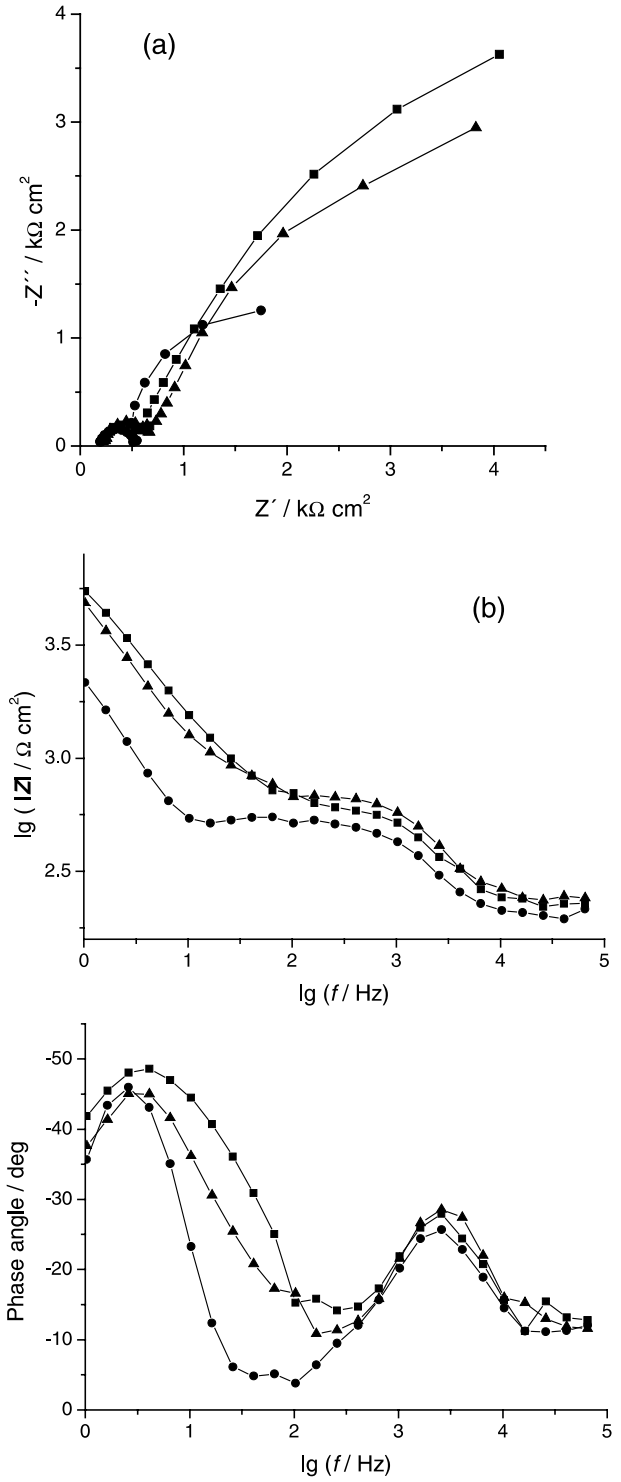

Fig. 5. Electrochemical impedance spectra at open circuit potential for aluminium. Immersion times: (■) 10 min, (●) 25 min and (▲) 60 min. Ultrasound applied between 12 and 17 min after immersion (2 s on + 1 s off). Ultrasound power 44 W cm^{-2}, tip–electrode distance 1.0 cm, $[Cl^-] = 0.1$ M, 3 mm diameter tip. (a) Complex plane plot; (b) Bode plots.

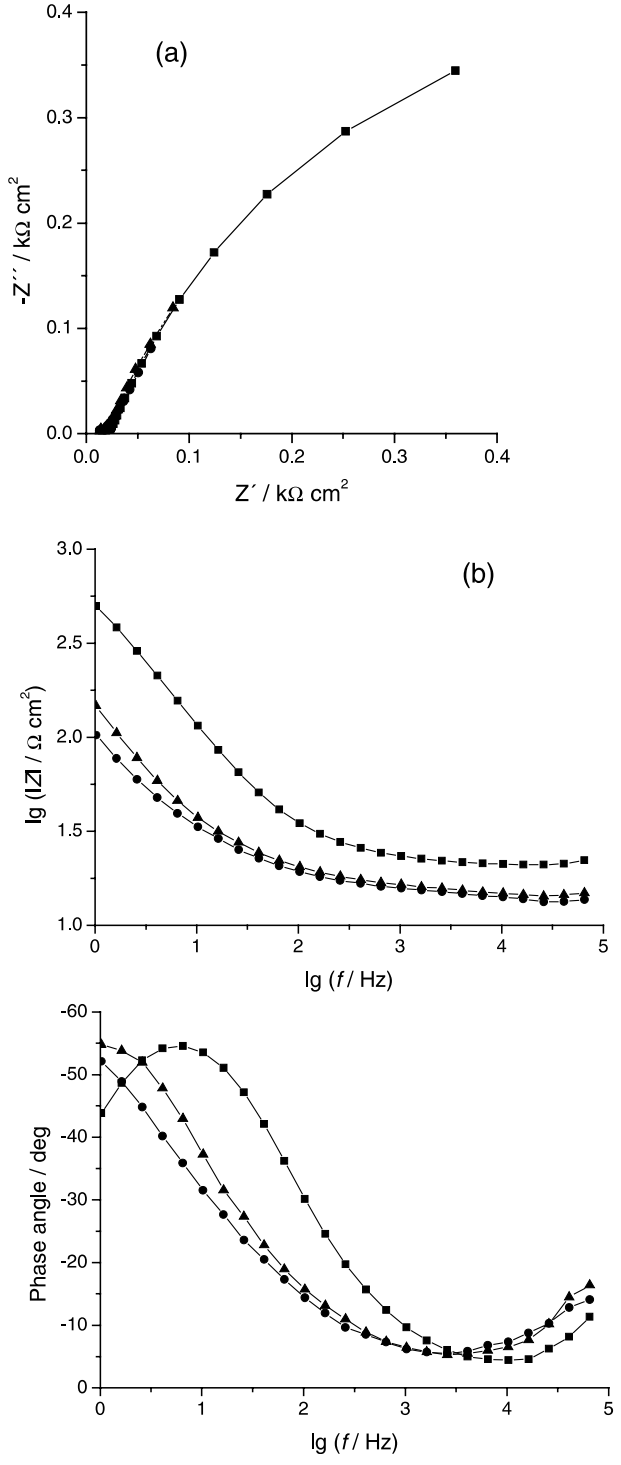

Fig. 6. Electrochemical impedance spectra at open circuit potential for high speed steel. Immersion times: (■) 10 min, (●) 25 min and (▲) 60 min. Ultrasound applied between 12 and 17 min after immersion (2 s on + 1 s off). Ultrasound power 44 W cm^{-2}, tip–electrode distance 1.0 cm, $[Cl^-] = 0.1$ M, 3 mm diameter tip. (a) Complex plane plot; (b) Bode plots.

The capacity values (*DE1*) also recover towards preirradiation values in the case of aluminium. However, for HSS the values of C_1 are much smaller and there is an irreversible change, with an increase in the value of capacity, after application of ultrasound which continues from 25 to 60 min, corresponding to the lack of a fast-formed stable robust oxide film.

Surface roughness of aluminium as expressed by the exponent α_1 is, within experimental error, lower after ultrasound (25 min) and essentially unchanged on

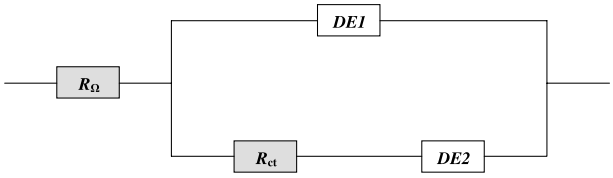

Fig. 7. Equivalent electrical circuit used to fit impedance spectra. R_Ω cell resistance, R_{ct}, charge transfer resistance at metal–electrolyte interface, DE1 and DE2, distributed elements modelled as CPEs.

comparing 10 min with 60 min immersion. However, α_1 is changed significantly for HSS and continues to fall. This reflects alterations to the surface which must be occurring.

The observed variations of both C_1 and α_1 suggest that there have been irreversible changes to the surface morphology and lead towards the same type of explanation advanced by Soyama [21] for situations in which the metal dissolution is rate-limiting.

3.5. *Scanning electron microscopy*

Micrographs of the surface before and after ultrasound-assisted corrosion can aid in elucidating the nature of the corrosion processes. Aluminium tends to form corrosion pits over the whole of the exposed surface area in an arbitrary way, as exemplified in Figure 8(a). These pits are not spherical, are relatively deep, and there is no evidence of the crystallographic etching, which occurs in quiet or only slowly moving solution [23]. Regarding high speed steel, Figure 8(b), the pits are smaller and more numerous. The ring of corrosion products formed on the top of the surface is similar to that observed in the absence of ultrasound; corrosion is primarily of the ferritic phase leaving the other alloying elements, which are mainly present as carbides [24].

3.6. *Comparative remarks*

The different techniques employed in this study have all clearly shown the effect of ultrasound on corrosion processes. The cavitation, and consequent bubble collapse, causes cleaning and erosion of the surface, which together with increased mass transport leads to pit formation and changes in the corrosion potential. Polarization curves and impedance spectra recorded nearly 10 min after application of ultrasound show the effects of surface changes.

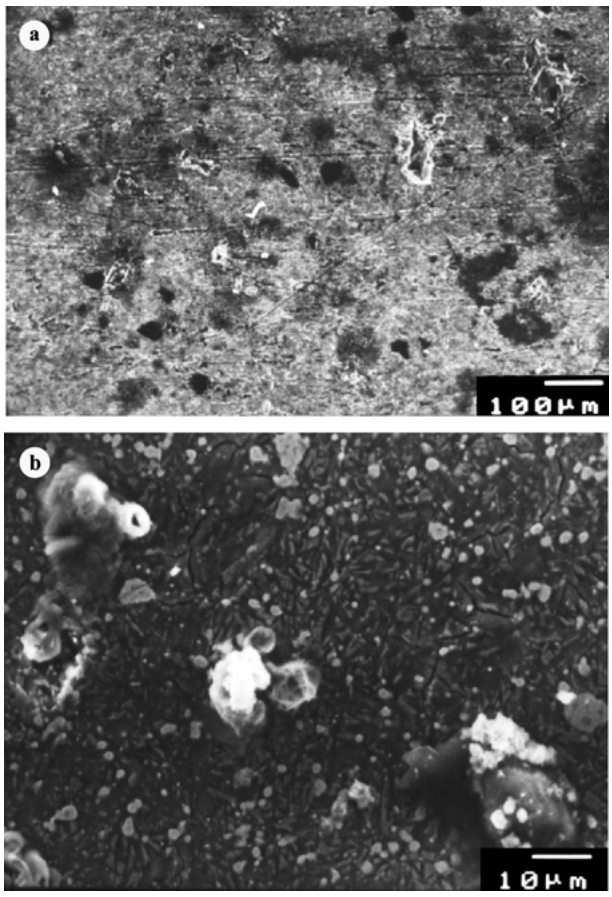

Fig. 8. Examples of scanning electron microscopy. (a) Aluminium and (b) high speed steel, after application of ultrasound for 5 min (2 s on + 1 s off): ultrasound power 44 W cm^{-2}, tip–electrode distance 1.0 cm, [Cl$^-$] = 0.1 M, 3 mm diameter tip.

The two metallic materials chosen for this study, aluminium and high speed steel, have different rate-limiting steps in the corrosion process. In the case of aluminium, where an oxide film is easily formed and the cathodic reaction is rate-limiting, ultrasound removes the oxide film, at least partially, and leads to formation of nonspherical deep pits. Nevertheless, the surface is able to recover from this action and reform an oxide

Table 4. Fitted values of circuit parameters from impedance spectra at different immersion times before and after ultrasound irradiation, using the equivalent circuit in Figure 7

	R_Ω/Ω cm^2	R_{ct}/Ω cm^2	C_1/μF cm^{-2}	α_1	C_2/μF cm^{-2}	α_2
Aluminium						
10 min	22	420	2.43	0.76	3.43	0.85
25 min	22	336	2.50	0.72	3.54	0.90
60 min	24	400	2.57	0.77	3.46	0.82
HSS						
10 min	22	1070	0.21	0.78	–	–
25 min	16	700	0.31	0.67	–	–
60 min	15	936	0.37	0.64	–	–

layer afterwards, so long as the chloride concentration is sufficiently low. If the concentration of chloride ion is too high, the ultrasound has very little effect in comparison to the aggressive chloride ion which is able to react with, and prevent the formation of, the passive film.

For high speed steel, where the metal dissolution reaction – primarily iron [24] – is rate dominating, ultrasound erodes the surface and causes it to return to a state similar to that on immersion except that pits are formed. Since there is no robust oxide film formation these permanent morphology changes are reflected in the subsequent behaviour of the steel samples; such irreversible alterations were noted by Soyama for carbon steel [21]. Permanent changes are also evident from the capacity changes seen in the electrochemical impedance spectra.

It is interesting to compare the results obtained with those of Man et al. [11] in which they studied a number of different engineering alloys, including different steels. The conditions they used for ultrasound application were rather different (i.e., 3.5% NaCl solution), applying ultrasound continuously over 4 h. Nevertheless, they too showed examples of effects of ultrasound changing the open circuit potential in a positive or negative direction depending on the relative importance of corrosion film and product removal and increase in mass transport. The different parameters which influence the corrosion process, under the experimental conditions employed, show that ultrasound power is clearly the most important.

The ultrasound-induced corrosion and erosion of the surface can certainly represent an accelerated corrosion test for metallic substrates such as aluminium which reform an oxide film afterwards or where, for high chloride concentration, the effect is essentially only an increase of mass transport. For other types of substrate, represented here by high speed steel, there are some irreversible changes to the surface which, if significant, mean that ultrasound cannot be used in such cases as an accelerated corrosion diagnostic to mimic ordinary corrosion tests over long time periods. Nevertheless, despite this possible drawback it can represent a valuable way for initial screening of corrosion resistance and given the widespread use of ultrasonic baths and other equipment an investigation of the mechanisms of corrosion in the presence, and as a consequence, of ultrasound is clearly of interest.

4. Conclusions

It has been demonstrated through electrochemical techniques and scanning electron microscopy that ultrasound increases the rate of corrosion of aluminium and high speed steel and leads to formation of pits in the surface. Aluminium, owing to its oxide forming ability, recovers from the application of ultrasound in terms of corrosion rate whereas high speed steel shows a small change.

Concerning the influence of ultrasound parameters on the corrosion rate in this study, with the 20 kHz horn probe, and for chloride ion concentrations not more than 0.1 M, that of the ultrasound power is greatest, followed by the distance between probe tip and metal, [Cl^-] and finally the area of the probe tip.

The potentiality of ultrasound-assisted corrosion as a rapid diagnostic test of corrosion resistance is demonstrated.

References

1. N. Moriguchi, *J. Chem. Soc. Jpn.* **55** (1934) 349.
2. G. Schmid and L. Ehret, *Z. Elektrochem.* **43** (1937) 408.
3. A.N. Karimov, V.A. Zakharov, L.I. Pleskach, F.S. Bekmukhametova and N.S. Sharipova, *Anal. Khim.* **46** (1991) 1983.
4. M.C. Hsiao and C.C. Wan, *Plat. Surf. Finish.* **76** (1989) 46.
5. R. Walker and C.T. Walker, *Ultrasonics* (1975) 79.
6. D. Juergen and E. Stekhan, *J. Electroanal. Chem.* **333** (1992) 177.
7. D.J. Walton and S.S. Phull, *Adv. Sonochem.* **4** (1996) 205.
8. R.G. Compton, J.C. Eklund and F. Marken, *Electroanalysis* **9** (1997) 509.
9. T.J. Mason and J.P. Lorimer, 'Sonochemistry: Theory, Applications and Uses of Ultrasound in Chemistry' (Ellis Horwood, Chichester, 1988).
10. M-L. Doche, J.-Y. Hihn, F. Touyeras, J.P. Lorimer, T.J. Mason and M. Plattes, *Ultrason. Sonochem.* **8** (2001) 291.
11. C.T. Kwok, F.T. Cheng and H.C. Man, *Mater. Sci. Eng.* A **290** (2000) 145.
12. A. Neville and B.A.B. McDougall, *Wear* **250** (2001) 726.
13. C.T. Kwok, F.T. Cheng and H.C. Man, *Surf. Coat. Technol.* **145** (2001) 194.
14. C.T. Kwok, F.T. Cheng and H.C. Man, *Surf. Coat. Technol.* **145** (2001) 206.
15. C.T. Kwok, H.C. Man and F.T. Cheng, *Mater. Sci. Eng. A* **303** (2001) 250.
16. C.T. Kwok, F.T. Cheng and H.C. Man, *Surf. Coat. Technol.* **107** (1998) 31.
17. C.T. Kwok, F.T. Cheng and H.C. Man, *Mater. Sci. Eng. A* **290** (2000) 74.
18. H.C. Man, C.T. Kwok and T.M. Yue, *Surf. Coat. Technol. A* **132** (2000) 11.
19. H.C. Man, S. Zhang, T.M. Yue and F.T. Cheng, *Surf. Coat. Technol. A* **148** (2001) 136.
20. K.F. Tam, F.T. Cheng and H.C. Man, *Surf. Coat. Technol. A* **149** (2002) 36.
21. H. Soyama and M. Asahara, *J. Mater. Sci. Lett.* **18** (1999) 1953.
22. P. Diodati and G. Giannini, *Ultrason. Sonochem.* **8** (2001) 49.
23. C.M.A. Brett, I.R. Gomes and J.P.S. Martins. *J. Appl. Electrochem.* **24** (1994) 1158.
24. C.M.A. Brett and P.I.C. Melo, *J. Appl. Electrochem.* **27** (1997) 959.
25. T.J. Mason, J.P. Lorimer and D.M. Bates, *Ultrasonics* **40** (1992) 30.